Localised model-based active controlling of blood flow during chemotherapy to prevent nail toxicity and onycholysis

Localised Model-Based Active Controlling of Blood Flow During Chemotherapy to Prevent Nail Toxicity and Onycholysis

Youssef, A., D'Haene, M., Vleugels, J.,De Bruyne G., Aerts J.-M.

Abstract

Chemotherapy-induced nail toxicity is a widely spread phenomenon. Cooling hands and feet of patients can reduce blood flow to the figures and consequently reducing the amount of chemical agents reaching the nails. This paper is aiming at developing a model-based controller of the finger's skin temperatures and blood flow through the fingers to reduce the risk of nail toxicity during chemotherapy. Experiments were conducted to model the dynamic response of the fingers skin temperature and blood flow using an ad hoc experimental device. The device was designed to provide a localised cooling of the fingers. The experiments were performed on a homogeneous test group of 11 middle-aged women (35-55 years old) because this is the highest risk-group for breast cancer. The fingers' skin temperatures and blood flow were measured continuously. A second order discrete time transfer function (DTF) model was suitable (R^2 = 0.91 ± 0.18) in all the cases to model the dynamic responses of the fingers' skin temperatures. The model estimation results have shown that the *a*-and *b*-parameters were not only varying among different test subjects but also within the same subject and for the same finger at different times. The resulting models were employed in the designing of model-based Proportional-Integral-Plus (PIP) controller. Simulations of the closed-loop systems were performed based on the identified models for each test subject. The simulation results have shown that the designed controller is able to regulate the finger's skin temperatures tightly about the desired level and yet, is still quite simple to implement in practice. Controlled active cooling with an online parameter estimation algorithm and continuous feedback of the patient finger temperatures and blood flow is a promising solution to reduce nail toxicity during chemotherapy.

1 Introduction

Cytotoxic chemotherapy is one of the most commonly used treatments for different types and stages of cancer. It is used to treat all stages of breast cancer, before and after surgery or radiation therapy. However, none of the used cytotoxic drugs has the ability to distinguish between normal (healthy) cells and cancer cells, consequently, causing severe adverse side effects. A large number of chemotherapeutic agents can be responsible for the development of nail changes (e.g., colouring, brittleness, damages …) of which the most sever and painful change is the onycholysis (Figure 1). Onycholysis is the detachment of (a portion of) the nail plate from the nail bed, often preceded or accompanied by severe pain [1, 2]. Minisini et al., [3] reported that 44% of the patients treated with Taxanes (Taxol®; Bristol-Myers Squibb Company; Princeton, NJ, USA) have developed forms of nail toxicities.

Nail changes are usually transitory and often diminish during treatment and disappear completely after drug withdrawal. However, in some cases, they persist after discontinuation of the treatment. Although nail changes are not life threatening, they should be managed properly since they can cause huge discomfort for the patient and even can be the cause of early discontinuation of the chemotherapy [4]. According to Can et al., [5], management of nail toxicity involves counselling patients regarding the potential for nail toxicity, providing practical strategies (nail cutting, avoiding potential irritants) for prevention, and instituting appropriate treatment (antibiotics) when necessary. Similar to the management of alopecia, nail toxicity can also be dealt with by *Cryotherapy* [5–7]. This

effect is related to a cold-induced vasoconstriction (CIVC), which reduces the amount of drug reaching the nails during the chemotherapy.

To prevent nail toxicity and onycholysis, cryotherapy is often applied by using frozen gloves and socks (Elasto-Gel©), or ice baths. By cooling the extremities, local vasoconstriction occurs, resulting in a reduction of the blood flow towards the fingers (and toes). Hence, the drugs cannot reach the nail bed that easily. However, the currently applied techniques are unpractical, uncomfortable and even painful, and often refused by the patients involved. Another important drawback of the cooling devices (ice bath or frozen gloves) is the fact that the temperature cannot be controlled and increases rapidly after putting on the cooling devices. The problem is even more complicated since the localised cooling of the extremities temporarily decreases the blood flow through the fingers/toes' blood vessels. However, as a counter reaction to prevent cold-induced damages to the fingers/toes, cold induced vasodilation (CIVD) will occur, which is called 'hunting phenomenon or Lewis reaction' [8, 9]. This will result in a sudden increase of the blood flow through the fingers/toes and consequently an increase of the skin temperature of the fingers/toes [10].

Hence, the ultimate objective of this research work is to introduce an actively controlled localised cooling technique of the fingers (and toes), that is able to decrease the blood flow through the fingers and yet avoid the cold-induced damages and sudden vasodilation (CIVD). The (r)evolution in modern sensing and computing technologies (price, compact size, flexibility and stretchability) is making it possible to continuously measure signals (e.g., body temperature at different parts) in real-time from human body using wearable technologies. That is giving the possibility to integrate sensors (e.g., finger temperatures) and actuators (e.g., localise cooling/heating) in an equipped gloves, for example, to actively control [11] the finger temperatures and consequently the blood flow.

This paper is aiming at developing a model-based controller of the finger's skin temperatures and blood flow through the fingers to reduce the risk of nail toxicity during chemotherapy. More specifically, it is aimed at modelling the dynamic response of the finger's skin temperatures to localise cooling, developing of model-based control system for skin temperature and simulating the controller performance.

2 Materials and Methods

2.1. Controllable active cooling device (iGlove-1) and measurements

An in-house (University of Antwerp, Belgium) developed active localised cooling device (*iGlove-1*, Figure 2) was developed to investigate the possibility of localised active cooling of hand fingers [12]. The *iGlove-1* device was developed in such way that it al-lowed to provide a stable localised low temperature (cooling) to the five fingers of the subject's left hand. The *iGlove-1* was equipped with 20 *Peltier* elements (two elements positioned on both sides of each finger) to establish localised cooling of the fingers. Each element is sized about 12 × 12 × 5 mm. The *iGlove-1* device consisted of a wooden construction on which the left subject's left hand can rest. The construction was equipped with five mechanically adjustable holders to ensure a good contact between the Peltier elements and the fingers of different hand sizes. The two Peltier elements located on each side of the finger (two on the fingertip and another below the first phalanx, Figure 2) are always electrically connected in series. Each Peltier element is equipped with its own Negative Temperature Coefficient (NTC) temperature sensor for feedback of the element's temperature to the controller. Schematic overview of the control system of the *iGlove-1* device is depicted in Figure 3. An Arduino-based Proportional-Integral-Differential (PID) controller is used to handle the amount of electrical power delivered to the Peltier

elements (for more information see [10, 11]). The finger's skin temperature, measured by the NTC sensor, is fed-back to the PID controller, together with the desired temperature (T_d) provided by the user via an ad-hoc PC-software interface. The PID controller is running on an Arduino-based hardware interface [12].

The *iGlove-1* device is equipped with five NTC sensors (with an accuracy of ±0.1 °C) to continuously measure the temperatures of the left-hand fingers. Another 20 NTC sensors are measured the temperature of the *Peltier* elements (one sensor for each element). A Laser Doppler blood flow meter (MoorVMS-LDF2® by Moor Instruments) was used to measure the changes in the blood flow underneath the nail bed. The blood flow measurements were performed on only two fingers, the index finger and the thumb, of the subject's left hand as a representation of the changes in the blood flow to the five fingers.

The temperature sensors were positioned on the underside of each fingertip, while the probes of the Laser-Doppler blood flow meter were placed on the middle of the nails of the thumb and index fingers. Skin temperatures of the five fingers and the ambient air (in degree Celsius, °C) were recorded, as well as the blood flow (in Perfusion Unit, PU) of the thumb and the index finger, every second.

2.2. Experiments

All the experiments and the experimental protocol were approved by the Ethical Committee of KU Leuven October 2014. In total, 33 experimental trials were conducted during the course of this study.

2.2.1. Test subjects

A homogeneous group of 11 healthy women between the ages of 35 and 55 years (given in Table 1) performed the tests. This age range was chosen since a high incidence rate of breast cancer is recorded within this age interval given the fact that chemotherapy is often applied for premenopausal women.

During the course of the experiments, all the test subjects were in a healthy conditions, non-smokers, having no hand injuries and with no evidences of *Perniosis* or *Raynaud* phenomenon. No (excessive) alcohol consumption by the all the test subjects was insured starting from the evening (6-8 pm) before the test with a normal (7-9) hours of sleep during night.

2.2.2. Experimental protocol

Acclimatisation stage: at the start of the measurements, each test subjects was seated in the test room for ±30 minutes to acclimatise to the, continuously measured, ambient air temperature (22.4 ± 0.6 °C) within the test room.

Step experiment stage: after placing the subject's left hand fingers in their appropriate positions on the *iGlove-1* device (Figure 2), the set-point temperature to the controller of the Peltier elements was set to 20 °C for 15 minutes. For another 30 minutes, a step-down decrease in the temperature of the Peltier element was applied by setting the controller set-point to 2 °C. These applied set-points were chosen in such way to insure that both the CIVC and CIVD phenomenon are triggered [12].

For each test subject, the previous test protocol was repeated three times in three consecutive days at the time of the day given in total 33 full experimental trials.

2.3. System identification

To design a model-based active control system for the fingers' skin temperature, a linearized representation of the system is required. Although the system under study (the finger/blood circulation) is inherently a non-linear system, the essential perturbation behaviour can often be approximated well by simple linearized Transfer Function (TF) models [11–17].

For the purposes of the present paper, therefore, the following liner, single-input, single-output (SISO) discrete-time-system was considered,

$$y(k) = \frac{b_1 z^{-1} + \cdots + b_m z^{-m}}{1 + a_1 z^{-1} + \cdots + a_n z^{-n}} u(k-\delta) + \xi(k) = \frac{B(z^{-1})}{A(z^{-1})} u(k) + \xi(k) \quad (1)$$

where $y(k)$ is the finger's skin temperature (°C) and $u(k)$ is the temperature of the Peltier elements (°C), while $A(z^{-1})$ and $B(z^{-1})$ are appropriately defined polynomials in the backshift operator z^{-1}, i.e., $z^{-i}y(k) = y(k-i)$ and $\xi(k)$ is additive noise, a serially uncorrelated sequence of random variables with variance σ^2 that accounts for measurement noise, modelling errors and effects of unmeasured inputs to the process (assumed to be a zero mean). For convenience, any pure time delay of $\delta > 1$ samples can be accounted for by setting the $\delta - 1$ leading parameters of the $B(z^{-1})$ polynomial to zero, i.e. $b_1, \cdots, b_{\delta-1} = 0$.
A step-input was applied, as explained earlier, by suddenly decreasing the temperature of the Peltier elements from 20 to 2 °C. In practice, the transition of the input to the new steady state is taking some times (transition time). However, for convenience, in this paper the step-input was idealised and normalised by assuming that it starts from zero and changes instantaneously at time equal zero,

$$\text{i.e., } u(t) = \begin{cases} 0 \; for \; t < 0 \\ 1 \; for \; t \geq 0 \end{cases} \quad (2)$$

The Simplified Refined Instrumental Variable (SRIV) algorithm was utilised in the identification and estimation of the models (model parameters and model structure) [18-19].

Firstly, the appropriate model structure was identified, i.e., the most appropriate values for the triad $[n,m,\delta]$ (see equation 1). Two main statistical measures were employed to determine the most appropriate values of these triad. Namely, the coefficient of determination R_2^T, based on the response error; and YIC (Young's Information Criterion), which provides a combined measure of model fit and parametric efficiency, with large negative values indicating a model which explains the output data well and yet avoids over-parameterisation [19-20].

2.4. Non-Minimal State Space (NMSS) formulation and model-based Proportional-Integral-Plus (PIP) controller design

This paper is discussing the design of an active control system for finger's skin temperatures and consequently, controlling the CIVC, using the temperature of the Peltier elements as control input. The PIP controller can be interpreted as a logical extension of the conventional Proportional-Integral/Proportional-Integral-Differential (PI/PID) controllers, with the advantage of additional dynamic feedback and input compensators, which are introduced automatically when the process has second order higher dynamics, or pure time delays greater than one sampling interval (which is the case in the process presented in this paper). Additionally, by

formulating the non-minimal state space (NMSS) models, directly from the identified models (see section 2.4.), the full state variable feedback can be implemented directly from the measured input and output signals (i.e., the controller design is automatically adopted when the model parameters and/or structure are changing online in closed-loop)..

The following methodology approach has been successfully used in earlier research work [16, 22], in which the NMSS model is formulated so that the full state feedback can be implemented directly from the measured input and output signal of the controlled process[22, 24].

Hence, the TF model (1) can be represented by the following NMSS equations [28],

$$\left.\begin{aligned} x(k) &= \mathbf{F}x(k-1) + \mathbf{g}u(k-1) + \mathbf{d}y_d(k) \\ y(k) &= \mathbf{h}x(k) \end{aligned}\right\} \quad (3)$$

where $x(k)$ is the $(n+m)$ dimensional non-minimal state vector, that is containing the present and the past sampled values of the output variable $y(k)$,the past sampled values of the input variable $u(k)$ and the integral of error between the reference (or command) input $y_d(k)$ and the sampled output variable $y(k)$. $\mathbf{F}$, $\mathbf{g}$, $\mathbf{d}$ and $\mathbf{h}$ are the state transition matrix, input vector, command vector and output vector, respectively [28]. The state variable feedback (SVF) control law associated with the NMSS model (3) takes the form:

$$u(k) = -\boldsymbol{k}^T x(k) \quad (4)$$

where $\boldsymbol{k}$ is the $(n+m)$ dimensional SVF control gain vector:

$$\boldsymbol{k}^T = [f_0 \;\; f_1 \;\cdots\; f_{n-1} \;\; g_1 \;\; \ldots \;\; g_{m-1} \;\; -k_1] \quad (5)$$

where f_0 and k_I are the proportional and integral actions, respectively, which are enhanced by higher order input and feedback compensators $G(z^{-1})$ and $F_1(z^{-1})$, respectively, and are defined as follows,

$$\boldsymbol{F}_1(z^{-1}) = f_1 z^{-1} + \cdots + f_{n-1} z^{-(n-1)},$$

$$\left.\begin{aligned} \boldsymbol{F}(z^{-1}) &= f_0 + f_1 z^{-1} + \cdots + f_{n-1} z^{-(n-1)} \\ \boldsymbol{G}(z^{-1}) &= 1 + g_1 z^{-1} + \cdots + g_{m-1} z^{-(m-1)} \end{aligned}\right\} \quad (6)$$

3. Results and discussions

3.1. Cold induced vasoconstriction (CIVC) and Cold induced vasodilation (CIVD)

Supporting the findings of previous studies [e.g., 12], data from 10 test subjects, out of 11 (test subject s11 did not show a clear response), have shown an evidence of CIVC (with average decrease in finger's skin temperature of 10.2 ±1.8 °C and average decrease in blood flow rate of 320 ±92 PU) due to applying the localised cooling. The measured blood flow of the 10 subjects, in both the index and the thumb fingers, have shown a decreasing pattern with the decreased fingers' skin temperatures. The blood flow measurements have shown signal perturbations due to the high sensitivity of the device to the movements during the experiments. Therefore, a moving average filtering, with window size of 20 samples, was applied to the signals before processing. Example of the CIVC evidence is shown in Figure 4, where decreasing in blood flow (about 400 PU drop), coupled with a drop in the finger's skin temperature (about 15 °C), in response to step decrease in the temperature of the Peltier elements were noticed.

Evidences of CIVC followed by CIVD were noticed with some subjects. Figure 5 is showing an example of CIVD evidence coupled with a rewarming of the index finger's skin after its temperature was dropped due to CIVC.

From theoretical point of view, one can find it is more convenient to use the blood flow measurements as control output (i.e., controlled variable). However, due to the noticed motion-intolerance behaviour of the blood flow measurements, it was found more practically convenient in the present paper to use the finger's skin temperature was used as control output to indirectly manipulate the blood flow through the fingers.

3.2. Control model identification and parameter estimates

The SRIV algorithm combined with the YIC and R_2^T suggested, in general, that a second order (number of poles, n = 2) discrete-time TF models described the dynamic responses of finger's skin temperature to step-decreases in the input (Peltier element's temperature) most accurately (i.e., R_2^T = 0.92 ±0.0765 and YIC = -9.66 ±3.22). More specifically, the SRIV algorithm identified the following general discrete-time TF model structure,

$$y(k) = \frac{b_1 z^{-1} + \cdots + b_m z^{-m}}{1 + a_1 z^{-1} + a_2 z^{-2}} u(k - \delta) + \xi(k) \quad (7)$$

where number of zeros (m) and time delays (δ) were different from one finger to another within the same test subject or between different subjects. The number of zeros (m) were within the range of 2 and 8. Table 2 is showing the average intra-person (within the same test subject) b-parameter estimates for each test subject.

The model estimation results have shown that the a-and b-parameters were not only varying among different test subjects but also within the same subject and for the same finger at different times. One test person (s11) was left out of consideration because the Lewis reaction was significantly more profound in her case than for the other test persons. Figure 6 is showing the deviation in both a_1-and a_2-parameter estimates within the same finger (index finger) for each test subject.

When the same finger (index finger) is considered, the average value of the model's a_1-parameters was -2 ± 0.12 for the 10 considered test subjects. Whereas, the a_2-parameters showed an average value around 1 ± 0.12. When the a-parameters of different fingers of the same person are compared, a lower standard deviation (< 0.08) for both. To investigate the significance of inter-person and intra-person differences in a-parameters, Student's t-test was performed [29]. The t-test was performed at significance level 0.05. At significance level 0.05, no significant differences (with average p-value of 0.28 ±0.10) were found in a-parameters for the different fingers within the same test subject (intra-person). However, the differences in a-parameters, by comparing the thumb and middle fingers, among the different test subjects (intra-person) were found significant (average p-value < 0.05). On the other hand, by comparing the a-parameters of the index finger for each test subject, the intra-person differences were found to be not significant (average p-value < 0.05) except for test subject s10 the differences in both a-parameters were found significant (p-value > 0.05).

These variations in the model structure and parameter estimates (especially within b-parameters) are forming a challenge for designing an active control system. To overcome such challenge, an on-line system identification and parameter estimations algorithm, such as SRIV or optimal Refined Instrumental Variables (RIV), is suggested to be used in a closed-loop [22]. The finger's dynamic bioresponse (e.g., skin temperature and blood flow) are nonlinear, however, the approach

presented in this paper is based on online model-based modelling of the process under question assuming a piece-wise linearity of the system. This approach has been applied successfully to model and control bio-systems in many previous studies (e.g., [14], [16], [17] and [18]).

For convenience, the obtained models from the index fingers (of the 10 test subjects) were considered for the control design and analysis. Table 3 is showing the average (and ± standard deviation) a- and b-parameters and number of zeros (m) for the index fingers of the considered 10 test subjects.

To simplify the representation of the design and analysis of the control systems in this paper, a representative model structure (i.e., the model triad n,m and δ) was chosen to be used for designing the model-based PIP controller. Model structure denoted by [2 2 2], i.e., n = 2, m = 2 and δ = 2, was the most representative (with highest R_2^T and the most negative YIC values, see Table 4) structure describing the dynamic responses of index finger's skin temperature for the 10 test subjects.

Figure 7 is illustrating an example for the dynamic responses of the index finger skin temperature, for test subject s7, to step-decrease in the input. The response was best described by the following discrete-time TF model, whose structure can be denoted by the triad [2 2 2], with R_2^T = 0.996 and YIC = -12.53,

$$y(k) = \frac{0.011z^{-2} - 0.0015z^{-3}}{1 - 1.995z^{-1} + 0.995z^{-2}} u(k) \tag{8}$$

or in the following difference equation form,

$$y(k) = 1.995y(k-1) - 0.995y(k-2) + 0.011u(k-2) - 0.0015u(k-3) \tag{9}$$

where $a_1 = -1.995$, $a_2 = 0.995$, $b_2 = 0.011$ and $b_3 = -0.0015$

3.3. NMSS formulation and PIP controller design

3.3.1. Framework of calculation

The NMSS formulations were done for the 10 test subjects. However, to ease the explanation of the calculations, the following formulations are based on the identified model (8), for test subject s7, as an example for the framework of NMSS formulation and PIP controller design.

From equation (3), the $(n + m)$ non-minimal state vector, $x(k)$, for the TF model (8) is given by,

$$x(k) = [y(k) \quad y(k-1) \quad u(k-1) \quad u(k-2) \quad z(k)]^T \tag{10}$$

The NMSS in this case is based on five state variables, namely, $y(k)$, $y(k-1)$, $u(k-1)$, $u(k-2)$ and $z(k)$. Where $z(k)$ is integral-of-error between the reference (or command) input $y_d(k)$ and the sampled output variable $y(k)$, defined as follows,

$$z(k) = z(k-1) + y_d(k) - y(k) \tag{11}$$

The state transition matrix $\mathbf{F}$, input vector $\mathbf{g}$, command vector $\mathbf{d}$ and output vector $\mathbf{h}$ of the NMSS system [26] are subsequently defined in below, based on the TF model (8),

$$\mathbf{F} = \begin{bmatrix} 1.995 & -0.995 & 0.011 & -0.0015 & 0 \\ 1 & 0 & 0 & 0 & 0 \\ 0 & 0 & 0 & 0 & 0 \\ 0 & 0 & 1 & 0 & 0 \\ -1.995 & 0.995 & -0.011 & 0.0015 & 1 \end{bmatrix}$$

$$\mathbf{g} = [0 \quad 0 \quad 1 \quad 0 \quad 0]^T$$

$$\mathbf{d} = [0 \quad 0 \quad 0 \quad 0 \quad 1]^T$$

$$\mathbf{h} = [1 \quad 0 \quad 0 \quad 0 \quad 0]^T$$

Hence, the NMSS servomechanism (PIP) control model of TF (8) is as follows:

$$\begin{bmatrix} y(k) \\ y(k-1) \\ u(k-1) \\ u(k-2) \\ z(k) \end{bmatrix} = \begin{bmatrix} 1.995 & -0.995 & 0.011 & -0.0015 & 0 \\ 1 & 0 & 0 & 0 & 0 \\ 0 & 0 & 0 & 0 & 0 \\ 0 & 0 & 1 & 0 & 0 \\ -1.995 & 0.995 & -0.011 & 0.0015 & 1 \end{bmatrix} . \begin{bmatrix} y(k-1) \\ y(k-2) \\ u(k-2) \\ u(k-3) \\ z(k-1) \end{bmatrix} + \begin{bmatrix} 0 \\ 0 \\ 1 \\ 0 \\ 0 \end{bmatrix} u(k-1) + \begin{bmatrix} 0 \\ 0 \\ 1 \\ 0 \\ 0 \end{bmatrix} y_d(k) \quad (12)$$

and,

$$y(k) = [1 \quad 0 \quad 0 \quad 0 \quad 0]x(k) \quad (13)$$

From equations (5) and (6), based on TF model (8), the controller filters are defined as follows,

$$\mathbf{F}(z^{-1}) = f_0 + f_1 z^{-1}$$

$$\mathbf{G}(z^{-1}) = 1 + g_1 z^{-1} + g_2 z^{-2} \quad (14)$$

Hence, from equations (4) and (14), the PIP control law, in difference equation form, for the system understudy is given by:

$$u(k) = u(k-1) + k_I\big(y_d(k-1) - y(k)\big) - f_0\big(y(k) - y(k-1)\big) - f_1\big(y(k-1) - y(k-2)\big) - g_1\big(u(k-1) - u(k-2)\big) \quad (15)$$

3.3.2. PIP closed-loop transfer function

The closed-loop control system can be represented in TF form as follows [28],

$$y(k) = \frac{k_I B(z^{-1})}{(1-z^{-1})\big(G(z^{-1})A(z^{-1}) + F(z^{-1})B(z^{-1})\big) + k_I B(z^{-1})} y_d(k) \quad (16)$$

From equations (8), (14) and (15) the closed-loop control system can be represented in block diagram form by Figure 8.

Analysing the characteristic equation, the denominator of equation (16), of the closed-loop system under study has revealed that the closed-loop TF is 5th order. The five control gains were calculated, from the characteristic equation, by assigning the poles manually to desired location in the complex z-plane (self-adaptive PIP control system will be introduced in further studies).

One of the main advantages of the above design approach is that it is automatically accommodating with the multiple-time delays that were observed with the various identified TF models for the finger's skin temperatures for different test subjects. The presented PIP controller automatically handles a pure time delay by simply feeding back sufficient past values of the input variable (the temperature of the Peltier element) to span the time delay [26].

3.3.3. Control simulation

The incremental form of the PIP control law, equation (15), can be implemented (or simulated) directly by coding it in a digital computer or impeded system. For practical application and simulation, to avoid integral windup in the PIP controller, which caused by integration of control errors during periods of actuator saturation, equation (15) was employed with the following correction,

$$u(k) = \begin{cases} u_{min},\ when\ u(k) < u_{min} = -4 \\ u_{max},\ when\ u(k) > u_{max} = 20 \end{cases}$$

Simulations of the closed-loop systems were performed based on the identified models for each test subject. That by combining the identified model for each test subject and the PIP control algorithm in a closed-loop. A zero mean (μ = 0) white noise term with variance (σ) of 0.1 was added to both output $y(k)$ and input $u(k)$ signals to simulate the measurement and actuator noises, respectively. A simulation example of the closed-loop response of the designed PIP controller based on the TF model (8) of index finger's skin temperature for subject s7, in which all the poles were assigned at 0.95, is shown in Figure 9.

The response of the finger's skin temperature in the simulated closed-loop, using the designed PIP controller based on each identified model, was following the desired set-points tightly with almost no overshooting. Although, choosing the poles close to the unity (i.e., equal 1) was causing the system to slow down towards steady-state, but it was more secure to avoid overshooting, which was more appropriate for such application.

3.3.4. Robustness analysis

An important consideration in the designed model-based PIP control system was the robustness of the control system performance to uncertainty associated with the model parameters [26]. The robustness problem here was arisen because the control system in this paper was designed based on approximation models (with the structure [2 2 2]) for the index finger's temperature of each test subject. In which the estimated a- and b-parameters (i.e., a_1, a_2, b_2 and b_3) were varying from test subject to another as shown in Table 4. The robustness analysis for the designed PIP controller was performed using the Monte Carlo (MC) simulation approach. The MC analysis employed in the presented paper was based on parameter covariance matrix [26] generated by the parameter estimation algorithm, SRIV, used to model the index finger's skin temperature from the 10 considered test subjects. In other words, the model parameters for each realisation in the MC analysis were selected randomly from the estimated ranges (presented in Table 4) and then combined randomly to form 50 different model combinations.

The MC analysis with 50 realisations of the feedback PIP controllers (Figure 10), showed that the control design was robust (with zero per cent unstable realisation) to the uncertainty and variations that might be associated with the estimated model parameters (within the defined ranges). However, it should be noted the controller was designed based on an approximation model structure, denoted by the triad [2 2 2], that was assumed to be representative for the fingers of all test subjects. Hence, for robust implementation of the controller, it is suggested for future work to develop an on-line

model identification algorithm with self-adoptive PIP control system [30], that is capable of tracking rapid parameter changes. This self-adaptive system is based on an on-line Time-Variable-Parameter (TVP) version of the recursive estimation algorithm (e.g., SRIV), which can be implemented in a closed-loop form.

The developed localised-cooling device (iGlove-1), together with the model-based PIP control system, has shown a promising solution to actively regulate the cooling of the patient finger's tips during the chemotherapy sessions.

4. Conclusions

The ultimate goal of this research work is to develop localised cooling system to actively control finger's skin temperature and consequently the blood flow to the fingertip during chemotherapy. An in house developed active cooling device (*iGlove-1*) was developed to investigate the possibility of localised active cooling of hand fingers with continuous feedback from the finger's skin temperature. A group of 11 females of 35 – 55 years old participated in the series of experiments. The skin temperature at the tip of the five fingers of the left hand has been measured, together with the blood flow in the thumb and index finger. Localised cooling was applied by decreasing the temperature of the Peltier elements to 2 ^{o}C to model the dynamics responses of the finger's skin temperatures of each finger for each test subject. Except for one test subject (s11), the test group showed a typical hunting phenomenon. In which, evidence of CIVC (with average decrease in finger's skin temperature of 10.2 ±1.8 ^{o}C and average decrease in blood flow rate of 320 ±92 PU) followed by CIVD evidence were noticed. In general, second order discrete-time TF models were the best (i.e., with average R_2^T= 0.92 ±0.08 and YIC= -9.66 ±3.22) to describe the dynamic responses of finger's skin temperature for all the consider test subjects. No statistically significant (p-values <0.05) intra-person differences were found between the a-parameters for all the 10 considered test subjects. However, the inter-person differences between the a-parameters were found significant (p-values >0.05). On the other hand, except for test subject s10, the inter-person differences between the a-parameters for the index fingers were found not significant (average p-value < 0.05). To simplify the design and analysis of the PIP control system, the models from index finger only were considered. Model-structure denoted by the triad [2 2 2] was the most suitable (with average R_2^T= 0.82 ±0.05 and YIC= -8.25 ±6.14) to be a representative model-structure to design the model-based PIP control system. Monte Carlo (MC) analysis was employed with 50 realisations to test the robustness of the designed PIP control system against parameter perturbations and variations. Within the defined ranges of variations in the model parameters, the MC analysis showed that the designed model-based PIP controller was robust (i.e., with zero per cent unstable realisation) able to regulate the finger's skin temperatures tightly about the desired level. The developed localised-cooling device (iGlove-1), together with the model-based PIP control system, has shown a promising solution to actively regulate the cooling of the patient finger's tips during the chemotherapy sessions.

5. References

1. Nicolopoulos, J., & Howard, A. (2002). Docetaxel-induced nail dystrophy. *The Australasian journal of dermatology*, *43*(4), 293–6.
2. Roh, M. R., Cho, J. Y., & Lew, W. (2007). Docetaxel-Induced Onycholysis: The Role of Subungual Hemorrhage and Suppuration. *Yonsei Medical Journal*, *48*(1), 124.

3. Minisini, A. M. (2003). Taxane-induced nail changes: incidence, clinical presentation and outcome. *Annals of Oncology*, *14*(2), 333–337.

4. Scotte, F. (2005). Multicenter Study of a Frozen Glove to Prevent Docetaxel-Induced Onycholysis and Cutaneous Toxicity of the Hand. *Journal of Clinical Oncology*, *23*(19), 4424–4429.

5. Can, G., Aydiner, A., & Cavdar, I. (2012). Taxane-induced nail changes: Predictors and efficacy of the use of frozen gloves and socks in the prevention of nail toxicity. *European journal of oncology nursing : the official journal of European Oncology Nursing Society*, *16*(3), 270–5.

6. Katsimbri, P., Bamias, A., & Pavlidis, N. (2000). Prevention of chemotherapy-induced alopecia using an effective scalp cooling system. *European journal of cancer (Oxford, England : 1990)*, *36*(6), 766–71.

7. Ridderheim, M., Bjurberg, M., & Gustavsson, A. (2003). Scalp hypothermia to prevent chemotherapy-induced alopecia is effective and safe: A pilot study of a new digitized scalp-cooling system used in 74 patients. *Supportive Care in Cancer*, *11*(6), 371–377.

8. Lewis, T. (1930). Observations upon the reactions of the vessels of the human skin to cold. *Heart*, *15*, 177–208.

9. Tang, F., Yu, C., Li, S., Ni, K., & Wang, X. (2015). Measurement of Peripheral Blood Flow Volume with New Heat Transfer Method. *Journal of Medical and Biological Engineering*, *35*(5), 677–684.

10. Daanen, H. A. M. (2003). Finger cold-induced vasodilation: a review. *European journal of applied physiology*, *89*(5), 411–26.

11. Marzencki, M., Tavakolian, K., Chuo, Y., Hung, B., Lin, P., & Kaminska, B. (2010). Miniature Wearable Wireless Real-time Health and Activity Monitoring System with Optimized Power Comsumption. *Journal of Medical and Biological Engineering*, *30*(4), 227–235.

12. Bladt, L., Clercq, J., Janssens, T., Hulle, J., Vleugels, J., Aerts, J.-M., & Bruyne, G. (2015). Cold-induced vasoconstriction for preventing onycholysis during cancer treatment. *Extreme Physiology & Medicine*, *4*(Suppl 1), A60.

13. Steckel, J., Goethijn, F., & De Bruyne, G. (2013). A research platform using active local cooling directed at minimizing the blood flow in human fingers. In *Pervasive Computing Technologies for Healthcare* (pp. 81–84). IEEE.

14. Aerts, J. M., Berckmans, D., Saevels, P., Decuypere, E., & Buyse, J. (2000). Modelling the static and dynamic responses of total heat production of broiler chickens to step changes in air temperature and light intensity. *British poultry science*, *41*(5), 651–659.

15. Young, P. C. (1989). *Control and Dynamic Systems: Advances in Theory and Applications*. (C.T. Leondes, Ed.). Elsevier.

16. Young, P. C. (1998). Data-based mechanistic modelling of environmental, ecological, economic and engineering systems. *Environmental Modelling and Software*, *13*(2), 105–122.

17. Youssef, A., Dekock, J., Ozcan, S. E., & Berckmans, D. (2011). Data-Based Approach to Model the Dynamic Behaviour of Greenhouse Temperature. *Acta Horticulturae (ISHS)*, *893*, 931–938.

18. Youssef, A., Exadaktylos, V., & Berckmans, D. (2014). Modelling and quantification of the thermoregulatory responses of the developing avian embryo: Electrical analogies of a physiological system. *Journal of Thermal Biology*, *44*, 14–19.

19. Youssef, A., Exadaktylos, V., Ozcan, S. E., & Berckmans, D. (2011). Proportional-Integral-Plus (PIP) Control System for Individual Thermal Zones in a Small Ventilated Space. *ASHRAE TRANSACTIONS*, *117*, 48–56.

20. Youssef, A., Yen, H., Özcan, S. E., & Berckmans, D. (2011). Data-based mechanistic modelling of indoor temperature distributions based on energy input. *Energy and Buildings*, *43*(11), 2965–2972.

21. Young, P. C., & Jakeman, A. (1980). Refined instrumental variable methods of recursive time-series analysis Part III. Extensions. *International Journal of Control*, *31*(4), 741–764.

22. Young, P. C. (2011). *Recursive Estimation and Time-Series Analysis: An Introduction for the Student and Practitioner*. Springer.

23. Young, P. C., Chotai, A., & Tych, W. (1991, April 28). Identification, estimation and control of continuous-time systems described by delta operator models. Kluwer Academic Publishers.

24. Young, P. C., Behazadi, M. A., Wang, C. L., & Chotai, A. (1987). Direct digital and adaptive control by input-output state variable feedback pole assignment. *International Journal of Control*, *46*(6), 1867–1881. Retrieved from http://dx.doi.org/10.1080/00207178708934021

25. Young, P. C., Lees, M. J., Chotai, A., Tych, W., & Chalabi, Z. S. (1994). Modelling and PIP control of a glasshouse micro-climate. *Control Engineering Practice*, *2*(4), 591–604.

26. Taylor, C. J., Chotai, A., & Young, P. C. (1998). Proportional-integral-plus (PIP) control of time delay systems. *Proceedings of the Institution of Mechanical Engineers, Part I: Journal of Systems and Control Engineering*, *212*(1), 37–48.

27. Taylor, C. J. (1998). Continuous time Proportional-Integral-Plus (PIP) control with filtering polynomials. In *UKACC International Conference on Control (CONTROL '98)* (Vol. 1998, pp. 1391–1396). IEE.

28. Taylor, C. J., Young, P. C., & Chotai, A. (2013). *True Digital Control: Statistical Modelling and Non-Minimal State Space Design*. Chichester, UK: John Wiley & Sons Ltd.

29. Levine, D. M., Ramsey, P. P., & Smidt, R. K. (2001). *Applied Statistics for Engineers and Scientists: Using Microsoft Excel and Minitab*. Prentice Hall.

30. Young, P. C., Behzadi, M. A., & Chotai, A. (1988). Self-tuning and self-adaptive PIP control systems. IET Digital Library.

Table 1. Age and assigned ID number of the each test subjects (#s)

Test person (ID number)	s1	s2	s3	s4	s5	s6	s7	s8	s9	s10	s11
Age (year)	47	50	35	42	54	39	43	41	44	46	53

Table 2. The average (± standard deviation) b-parameter estimates, number of zeros (m) and delays (δ) per test subject (s#) with the average (± standard deviation) coefficient of determination R_2^T and YIC.

s#	$B(z^{-1})$								m	δ	R_T^2	YIC
	b_0	b_1	b_2	b_3	b_4	b_5	b_6	b_7				
1	0	0	0	-0.0122 ± 0.006	0.0712 ± 0.032	-0.237 ± 0.121	0	0	3	3	0.92 ± 0.04	-6.25 ± 2.12
2	0	0.1853 ± 0.023	0.3711 ± 0.086	0.1859 ± 0.075	0	0	0	0	3	1	0.95 ± 0.03	-11.20 ± 3.06
3	0	0	0	0.0014 ± 0.002	-0.0014 ± 0.002	0	0	0	2	3	0.98 ± 0.01	-10.20 ± 4.06
4	0.0008	0	0	0.1597 ± 0.080	0	0	0	0	2	0	0.94 ± 0.04	-11.08 ± 2.06
5	0	0	0	0.6226 ± 0.123	-1.8180 ± 0.202	1.7694 ± 0.45	-0.5740 ± 0.132	0	4	4	0.90 ± 0.05	-9.08 ± 2.06
6	1.0e-05	0	0	0	0	0.3337 ± 0.134	0	0	2	0	0.86 ± 0.06	-5.17 ± 1.78
7	0	0	0.012 ± 0.006	-0.0015 ± 0.001	0	0	0	0	0	2	0.96 ± 0.02	-10.18 ± 2.14
8	0.0002	0	0	0	0	0.972 ± 0.325	-0.968 ± 0.465	0	3	0	0.95 ± 0.03	-9.37 ± 3.45
9	0	0	0	0.0024 ± 0.002	-0.0023 ± 0.002	0	0	0	2	3	0.88 ± 0.05	-7.56 ± 4.04
10	0	0	0	0.0561 ± 0.008	-0.12 ± 0.523	0.0533 ± 0.007	0	0	3	4	0.96 ± 0.01	-11.23 ± 2.31

Table 3. Average and standard deviation of parameter estimates, R_2^T and YIC for index finger from the considered 10 test subjects.

$A(z^{-1})$		$B(z^{-1})$				m	R_T^2	YIC
a_1	a_2	b_0	b_1	b_2	b_3			
-1.985 ± 0.562	0.986 ± 0.610	0.0 ± 0.0	0.0012 ± 0.0002	-0.337 ± 0.349	-0.258 ± 0.221	3	0.91 ± 0.04	-7.25 ± 3.14

Table 4. Average (± standard deviation) a- and b-parameter estimates for the representative model structure, denoted [2 2 2], of the index finger's skin temperature for the 10 considered test subjects.

	$A(z^{-1})$		$B(z^{-1})$		R_T^2	YIC
	a_1	a_2	b_2	b_3		
Mean ± std	-1.993 ± 0.562	0.986 ± 0.610	-0.227 ± 0.329	-0.072 ± 0.176	0.86 ± 0.05	-8.25 ± 6.14
Min	-2.653	0.955	-0.015	-0.125	0.79	-13.20
Max	-1.955	1.655	0.112	0.131	0.99	-3.34

Figure 1. Example of haemorrhagic onycholysis. Development of the nail lesions can be associated with intense pain [3].

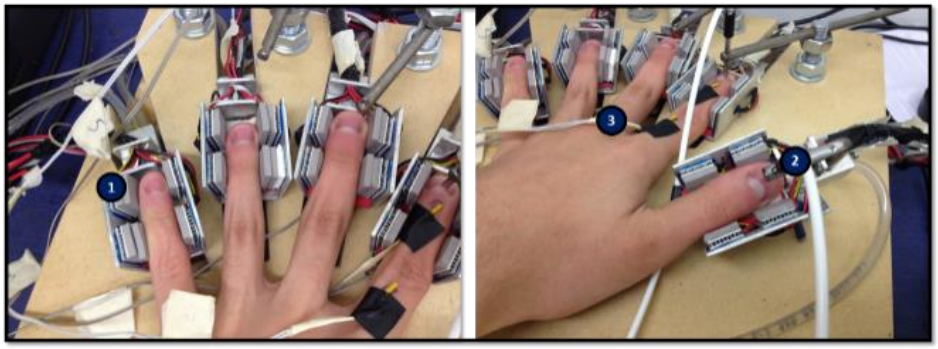

Figure 2. The *iGlove-1* controlled cooling device for the left hand. (1) Peltier cooling elements (2) one probe of the blood flow Laser Doppler meter (3) NTC temperature sensor to measure the finger skin temperature.

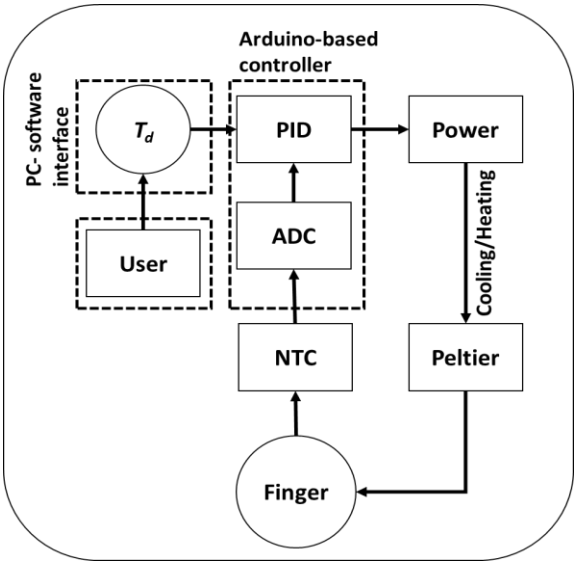

Figure 3. Schematic overview of the control system of the *iGlove-1* device [11]. A PID controller implemented using an Arduino-based hardware interface controls the electric power to the *Peltier* elements and consequently drives its temperature to the desired one (T_d). The temperatures of the elements is measured using an NTC sensors to be fed-back to the PIC controller after conversion to digital using an Analog-to-Digital Converter (ADC). All the data from and to the *iGlove-1* device is sent to the PC for further analysis.

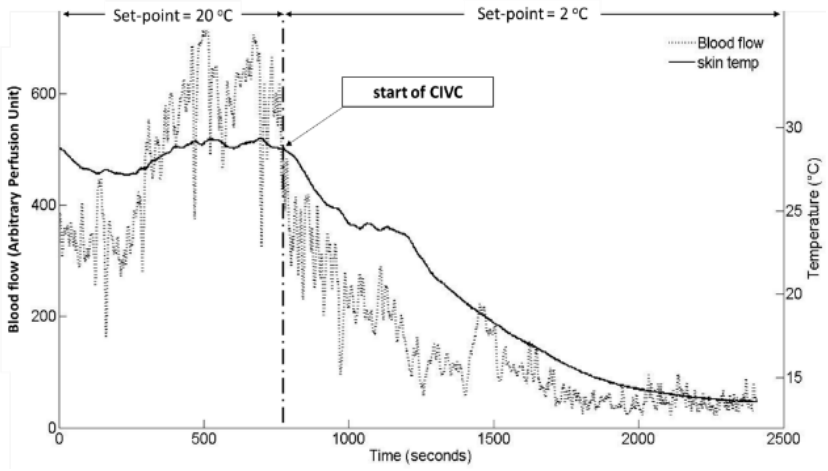

Figure 4. The coupled responses of blood flow to the index finger's skin (of subject #s4) temperature to step decrease in the Peltier elements temperatures (from 20 °C to 2 °C).

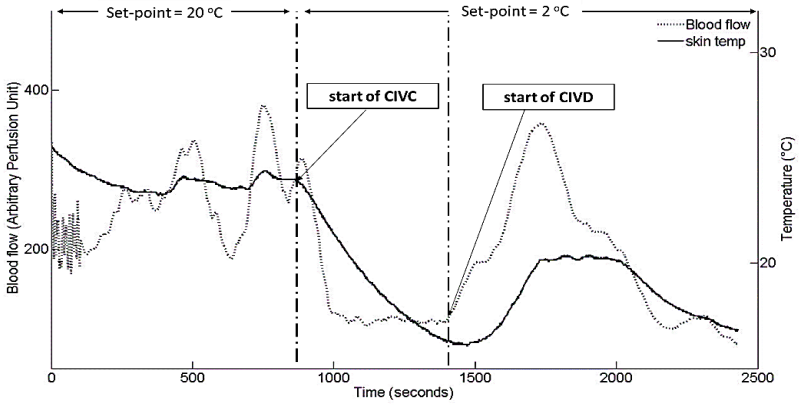

Figure 5. Example of an evidence of CIVC, coupled by a drop in the index finger's skin temperature, followed by CIVD causing rewarming of the finger's skin temperature (of subject #s6) in response to the step decrease in the temperature of the Peltier elements.

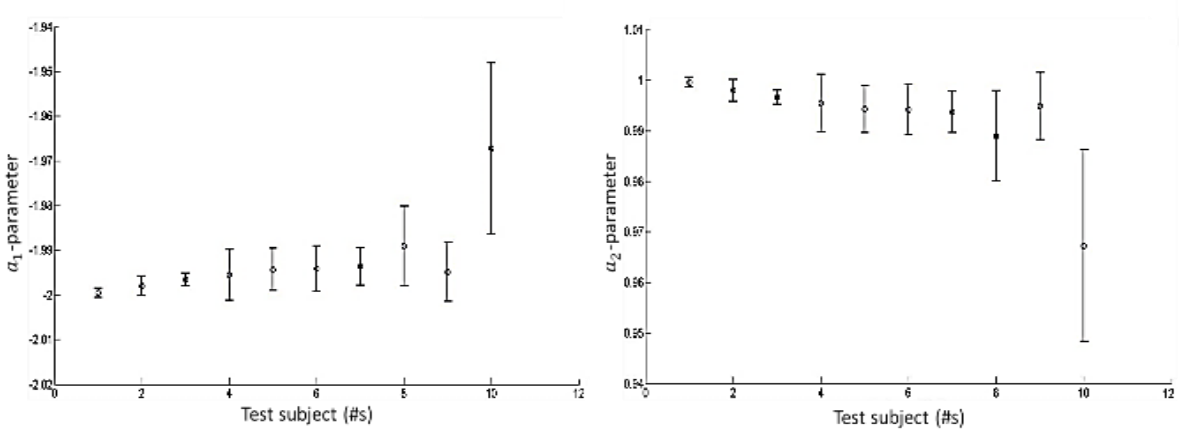

Figure 6. The mean and standard deviation of a_1-and a_2-parameters of the model estimates for each test subject based on measurements from their index fingers.

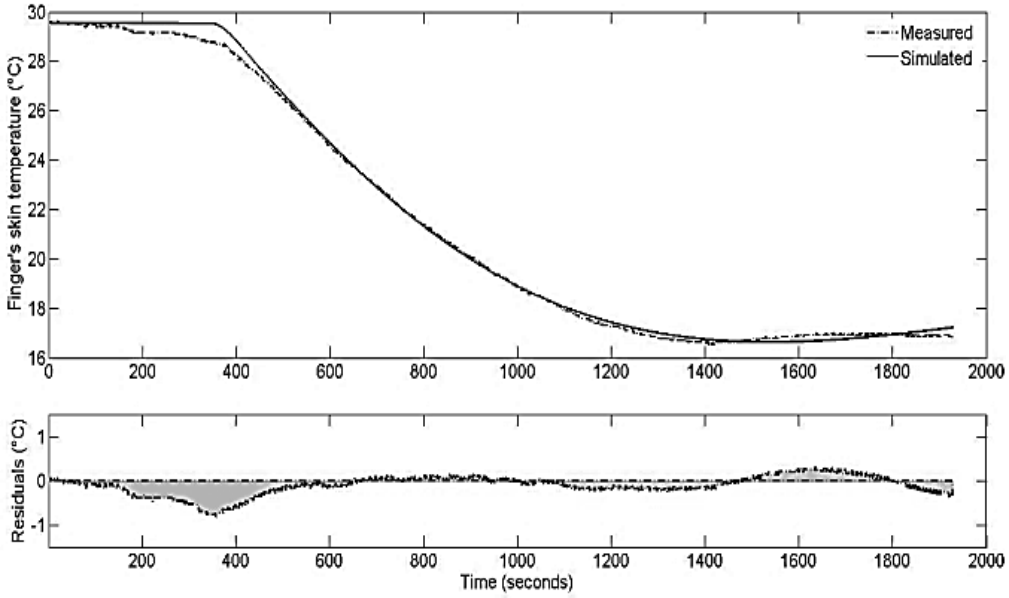

Figure 7. Example (from subject number s_7): modelled dynamic response of Finger's (index finger) skin temperature to step decrease in Peltier element temperature, shows a comparison between the measured and simulated temperatures and the residuals.

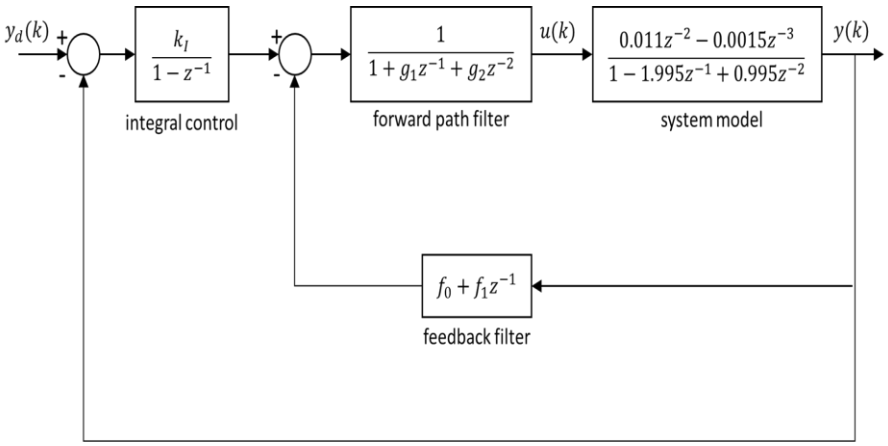

Figure 8. Block diagram of the closed-loop PIP control system based on TF model (8).

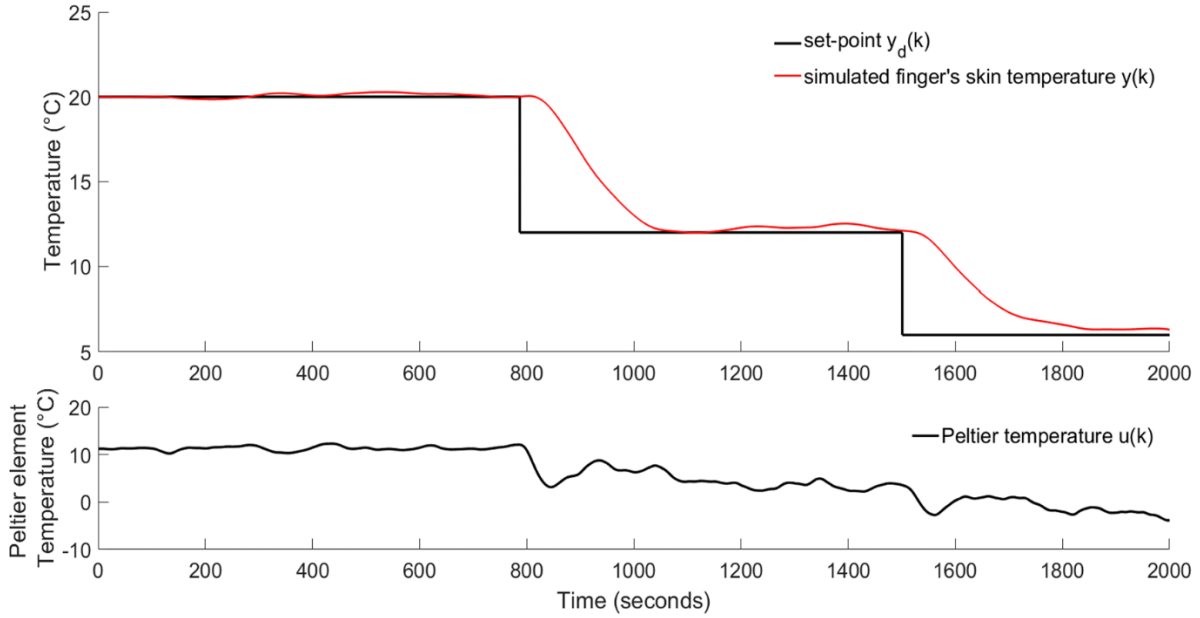

Figure 9. A simulation example of the~~Simulated~~ closed-loop step responses $y(k)$ (upper graph) using the designed PIP controller of the finger's skin temperature, showing the control input signal $u(k)$(lower graph).

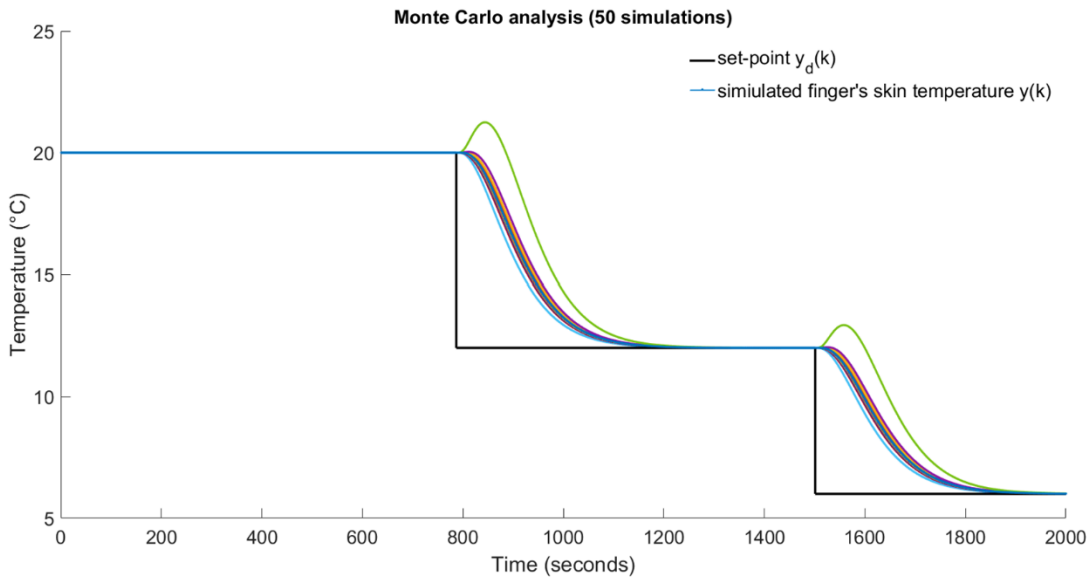

Figure 10. Monte Carlo responses of the various PIP controllers to a step changes in the command (set-point $y_d(k)$) input, with 50 Monte Carlo realisations.